Analysis of the ESR linewidth in pristine *trans*-polyacetylene

Kenji Mizoguchi, Shin-ichi Masubuchi,* and Kiyoshi Kume
Department of Physics, Tokyo Metropolitan University, Hachi-oji, Tokyo, 192-03 Japan

Kazuo Akagi and Hideki Shirakawa
Institute of Materials Science, University of Tsukuba, Tsukuba-shi, Tennodai, Ibaraki, 305 Japan
(Received 22 July 1994; revised manuscript received 31 October 1994)

The cw ESR linewidth was studied in detail as a function of frequency and temperature in pristine *trans*-$(CH)_x$ and $(CD)_x$ prepared by the Shirakawa technique. It was demonstrated that all the obtained data could be interpreted by quasi-one-dimensional diffusive motion of the neutral soliton with a diffuse-trap soliton model. An anomalous line broadening below 6 MHz was observed only in *trans*-$(CH)_x$. The origin was ascribed to a crossover from "unlike spins" to "like spins" as a relation between electron and nuclear spins. Such an interpretation gives the maximum spin density $\rho_{max} \approx 0.1$ of the delocalized neutral soliton. The temperature dependence of the motion-narrowed ESR linewidth $T_2'^{-1}$ was found to be consistent with the phase memory time T_M^{-1} in terms of the diffuse-trap model. It is discussed that direct evidence of the diffuse-trap model is given by multiple-quantum-spin coherence experiments, although the original authors concluded that all the solitons were trapped both at 4.2 and 300 K. The temperature dependence of the diffusion rate $D_\parallel$ along the polymer chain was found to follow a T^2 law. This behavior is consistent with that deduced from the NMR T_1 data. With this agreement between the two resonance methods, validity of the applied diffuse-trap model was reconfirmed. Another interpretation for $D_\parallel$ derived from ESR T_1 was discussed in connection with the present interpretation. The temperature dependence of the cutoff frequency $1/\tau_\perp$ was interpreted by exchange coupling between the solitons at low temperatures and a phonon-assisted hopping through the charged solitons at high temperatures, as discussed by Kivelson and Heeger.

I. INTRODUCTION

For more than ten years a prototype of conjugated polymer, "polyacetylene" has been studied from a lot of views as follows: improvements of quality of electrical and mechanical properties, investigations on electronic structures, especially elementary excitations of solitons theoretically expected in an intermediate doping regime, and a "metallic" conducting state in a heavily doped regime, dynamics of charge carriers, applications, especially on a light weight and high power organic batteries, and so on.[1] Among these points, a lot of magnetic resonance studies, NMR and ESR, have been done, focusing on the dynamics of the neutral soliton in pristine *trans*-polyacetylene.[1] The presence of a neutral soliton in *trans*-polyacetylene, as one of the systems with doubly degenerate ground state, was proposed theoretically by Su, Schrieffer, and Heeger (SSH).[2]

The first ESR experiment on soliton dynamics was done on the temperature dependence of an ESR linewidth at the X band by Weinberger *et al.* and low-dimensional rapid motion of the spin carrier was concluded.[3] The proton NMR has been studied as a function of frequency by Nechtschein *et al.* in 1980.[4] They concluded that the neutral soliton showed a rapid diffusion as high as 10^{13} rad/s in pristine *trans*-polyacetylene and that the charged spin carrier diffuses rapidly up to 10^{17} rad/s in AsF_6-doped conducting polyacetylene, nevertheless some ambiguity remained in their interpretation. These conclusions were confirmed by the Overhauser effect observed in the dynamic nuclear polarization (DNP) experiments.[5–7]

Furthermore, pulse ESR techniques were applied to investigate the soliton dynamics; ESR spin-lattice relaxation rate,[8] ESR spin-echo decay rate,[9] ESR free-induction decay shape[10] and multiple-quantum spin coherences.[11] A common qualitative conclusion derived from these pulsed ESR's was that the spin carrier in the pristine polyacetylene made some motion, but a consensus could not be achieved on a time scale of motion. This inconsistency among the pulse ESR data would strongly depend on their interpretations. For example, what the ESR spin-echo decay time sees is model dependent. The above-mentioned inconsistency among different kinds of experiments would be derived from different assumptions based on different models.

In this paper, we will show a detailed experiment and analysis of the ESR linewidth as functions of temperatures and frequencies based on a diffuse-trap model for the neutral soliton.[12–14] The present analysis of the ESR linewidth has revealed that the diffuse-trap model could give a consistent interpretation not only for the cw linewidth, but also for the reported pulsed ESR data,[8–11] including anomalous excess broadening of the linewidth found below 6 MHz not in *t*-$(CD)_x$, but in *t*-$(CH)_x$ which could be analyzed to be compatible with solitonlike charge distribution. Furthermore, multiple quantum coherence experiment provided a clear evidence for a presence of the neutral soliton in a trapping state. A quantitative result derived by the DNP technique will also be discussed in conjunction with the present model.

II. EXPERIMENT

Pristine *cis*-polyacetylene was prepared by the conventional Shirakawa method.[15] To obtain *trans*-form, thermal isomerization around 180–200 K was applied for more than 10 min. Samples for ESR and NMR measurements were sealed with helium gas for thermal contact in quartz tubes to avoid sample oxidation and degradation.

ESR linewidth was determined by applying a least-squares fitting to the experimental data with Lorentzian line shape. This method is indispensable at low magnetic field because a resonance field becomes smaller than the ESR linewidth. Even at 10 K and 3 MHz, the observed line shape was found to be a good Lorentzian. The number of Curie spins was determined by the Schumacher-Slichter (ESR-NMR) technique which does not require any external standard of the number of spins.

III. THEORETICAL BASIS OF SPIN-DYNAMICS STUDY

The spin-dynamics study measures the frequency spectrum of a local field produced by a rapid spin motion to investigate anisotropic motion of a spin carrier, as schematically represented in Fig. 1. If the spin carrier diffuses one-dimensionally (1D), the spins pick up the local magnetic field $H_{\rm loc}$ through electron-electron dipolar and/or electron-nuclear hyperfine couplings, modulated by the diffusive motion [Figs. 1(b) and 1(c)]. A Fourier spectrum $J(\omega_0)$ of the autocorrelation function $G(t)$ for $H_{\rm loc}$ [Fig. 1(d)] on resonance of the electron spins induces a transition between Zeeman levels, and as a result the spin system relaxes to a thermal equilibrium state, releasing and/or absorbing the Zeeman energy to and/or from a lattice through the electron spin motion.

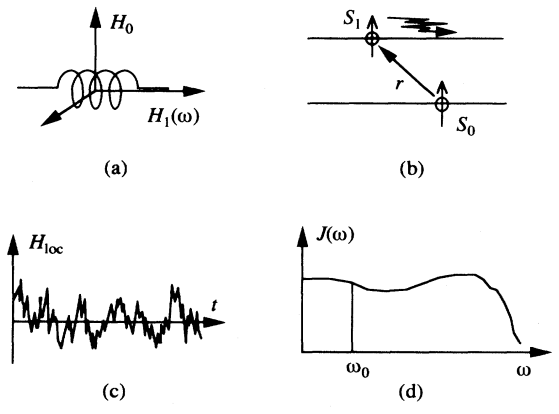

FIG. 1. Schematic explanations for the relaxation phenomena induced by motion of spin. (a) A setting of the rf coil and the static magnetic field H_0 for the magnetic resonance. (b) The relation of two spins diffusing on the one-dimensional chains. (c) The local magnetic field modulated randomly by the spin motion seen by the concerning spin as a function of the time. (d) The spectral density of the autocorrelation function of the local fluctuating magnetic field shown in (c).

A. Autocorrelation function of fluctuating local field

An expression for the autocorrelation function $G(t)$ is given by Abragam[16] as

$$G(t)=\int\int p(\mathbf{r}_1)\Phi(\mathbf{r}_1,\mathbf{r}_2,t)F(\mathbf{r}_1)F^*(\mathbf{r}_2)d\mathbf{r}_1 d\mathbf{r}_2 , \quad (1)$$

where $p(\mathbf{r}_1)$ is the probability density to find a spin at $\mathbf{r}_1$, that is, a spin concentration c, $\Phi(\mathbf{r}_1,\mathbf{r}_2,t)$ is the probability density for a spin initially at $\mathbf{r}_1$ to be found at $\mathbf{r}_2$ after the time t, which is governed by the dimensionality of spin motion as will be discussed later, and $F(\mathbf{r})$ is the random function of an implicit parameter t and is determined by a functional form of the interaction Hamiltonian $\mathcal{H}_1=\sum_q F^{(q)}A^{(q)}$, for example, in the case of the dipolar interaction,

$$A^{(0)}=-\tfrac{3}{2}\gamma_I\gamma_S\hbar\{-\tfrac{2}{3}I_zS_z+\tfrac{1}{6}(I_+S_-+I_-S_+)\} ,$$

$$F^{(0)}=\frac{1-3\cos^2\theta}{r^3} , \quad (2a)$$

$$A^{(\pm1)}=-\tfrac{3}{2}\gamma_I\gamma_S\hbar\{I_zS_\pm+I_\pm S_z\} ,$$

$$F^{(\pm1)}=\frac{\sin\theta\cos\theta e^{\mp i\varphi}}{r^3} , \quad (2b)$$

$$A^{(\pm2)}=-\tfrac{3}{4}\gamma_I\gamma_S\hbar I_\pm S_\pm , \quad F^{(\pm2)}=\frac{\sin^2\theta e^{\mp 2i\varphi}}{r^3} , \quad (2c)$$

where r is the length of the vector $\mathbf{r}$ connecting two spins, θ is the polar angle of $\mathbf{r}$ about H_0, and φ is the azimuthal angle about H_0.

Since the chains consist of discrete atoms or molecules in the actual systems, we redefine $G(t)$ by

$$G^{(j)}(t)=c\sum_{r_1,r_2}\Phi(\mathbf{r}_1,\mathbf{r}_2,t)F^{(j)}(\mathbf{r}_1)F^{(j)*}(\mathbf{r}_2) . \quad (3)$$

Then, the Fourier transform of $G(t)$ gives the spectral density $J(\omega)$ by

$$J^{(j)}(\omega)=c\sum_{r_1,r_2}\phi(\mathbf{r}_1,\mathbf{r}_2,\omega)F^{(j)}(\mathbf{r}_1)F^{(j)*}(\mathbf{r}_2) , \quad (4)$$

where $\phi(\mathbf{r}_1,\mathbf{r}_2,\omega)$ is the Fourier transform of the probability density $\Phi(\mathbf{r}_1,\mathbf{r}_2,t)$ and the sum is over r_1 and r_2 with all the possible sites.

B. Spectral density for 1D diffusion

If we consider the spins diffusing on a one-dimensional (1D) chain with a diffusion coefficient $\mathcal{D}_\parallel$(cm^2/s) or a diffusion rate $D_\parallel$ (rad/s) ($=\mathcal{D}_\parallel/c_\parallel^2$, $c_\parallel$ is the lattice constant), the probability density $\Phi_{\rm 1D}(\mathbf{r}_1,\mathbf{r}_2,t)$ is given by a solution of the 1D diffusion equation, $\partial\Phi/\partial t=\mathcal{D}_\parallel\Delta\Phi$, which is valid in the longer time scale than $1/D_\parallel$. It is well known that the solution of this equation is given by

$$\Phi_{\rm 1D}(r_1,r_2,t)=\frac{1}{\sqrt{4\pi D_\parallel t}}\exp\left[-\frac{(|r_1-r_2|/c_\parallel)^2}{4D_\parallel t}\right] . \quad (5)$$

Here, note that $D_\parallel$ should be replaced by $2D_\parallel$ for the electron-electron dipolar case where the spins diffuse mutually. Since the actual systems are more or less quasi-one-dimensional (Q1D), we need to take account of a cutoff of the 1D correlation of motion as the escape probability from the 1D chain by $\Phi_\perp(t)=\exp(-2t/\tau_\perp)$, where $\tau_\perp$ is the mean lifetime of the 1D correlation. Then, the probability density for the Q1D system can be given by

$$\Phi_{\mathrm{Q1D}}(r_1,r_2,t)=\Phi_{\mathrm{1D}}(r_1,r_2,t)\cdot\Phi_\perp(t)=\frac{\exp\{-2t/\tau_\perp\}}{\sqrt{4\pi D_\parallel t}}\exp\left[-\frac{(|r_1-r_2|/c_\parallel)^2}{4D_\parallel t}\right]. \tag{6}$$

An expected frequency dependence of the spectral density $J(\omega)$ for the quasi-one-dimensional diffusion is given by a Fourier transform of Eq. (6):

$$\phi_{\mathrm{Q1D}}(|r_1-r_2|,\omega)=\frac{1}{\sqrt{4D_\parallel/\tau_\perp}}\left[\frac{1+\sqrt{1+(\omega\tau_\perp/2)^2}}{1+(\omega\tau_\perp/2)^2}\right]^{1/2}\times\exp(-\eta u)\left[\cos(\eta v)-\frac{v}{u}\sin(\eta v)\right], \tag{7}$$

where

$$\eta=\frac{|r_1-r_2|}{c_\parallel}\left[\frac{2/\tau_\perp}{D_\parallel}\right]^{1/2},$$

$$u=\left[\frac{\sqrt{1+(\omega\tau_\perp/2)^2}+1}{2}\right]^{1/2},$$

and

$$v=\left[\frac{\sqrt{1+(\omega\tau_\perp/2)^2}-1}{2}\right]^{1/2}.$$

Although Eq. (7) is a complicated relation, we have a simplified formula

$$\phi_{\mathrm{Q1D}}(\omega)\approx\frac{1}{\sqrt{4D_\parallel/\tau_\perp}}\left[\frac{1+\sqrt{1+(\omega\tau_\perp/2)^2}}{1+(\omega\tau_\perp/2)^2}\right]^{1/2}, \tag{8}$$

for the scalar interaction[17] [$\propto\delta(r_1-r_2)$] and the dipolar interaction[18] under the condition $\eta u\ll 1$, i.e., $\omega\ll D_\parallel c_\parallel^2/\Delta r^2$, where Δr is the effective range of interaction. Actually, Δr falls within several Angstrom which is large enough to reduce the dipolar coupling strength to several % of its maximum by virtue of $1/(r_1^3r_2^3)$ dependence as shown in Eqs. (1) and (2). Therefore, $\eta u\ll 1$ approximately holds at all frequencies of $\omega\ll D_\parallel$ where the diffusion equation is valid. In the case of the delocalized wave function,[19] the r-dependent part in Eq. (6) plays a very important role to suppress the spectral intensity proportional to Eq. (7), especially in the case of ESR T_1^{-1} and T_2^{-1} at the X band and lower temperatures where $D_\parallel$ becomes small in the present analysis, as will be discussed in Sec. V F.

The basic behavior of the spectral density $J(\omega)$ can be described by Eq. (8) and the next two expressions valid in each frequency regime:

$$\phi_{\mathrm{Q1D}}(\omega)\approx\frac{1}{\sqrt{2D_\parallel\omega}}\quad\text{for } 1/\tau_\perp\ll\omega\ll D_\parallel, \tag{9a}$$

$$\phi_{\mathrm{Q1D}}(\omega)\approx\frac{1}{\sqrt{2D_\parallel/\tau_\perp}}=\text{const}\quad\text{for } \omega\ll 1/\tau_\perp. \tag{9b}$$

Equation (9a) demonstrates typical 1D behavior of $1/\sqrt{\omega}$ and (9b) does that of 3D, commonly found in the conducting polymers.

C. Spin-lattice T_1^{-1} and spin-spin T_2^{-1} relaxation rates

Expressions for T_1^{-1} and T_2^{-1} are given by

$$\begin{aligned}T_1^{-1}&=\tfrac{3}{2}\gamma_S^4\hbar^2S(S+1)[J^{(1)}(\omega_0)+J^{(2)}(2\omega_0)]\\&=\gamma_S^4\hbar^2S(S+1)c\sum_l[0.2\phi(\omega_0)+0.8\phi(2\omega_0)]\\&=3\gamma_S^2k_BT\chi\sum_l[0.2\phi(\omega_0)+0.8\phi(2\omega_0)],\end{aligned} \tag{10}$$

$$\begin{aligned}T_2^{-1}&=\tfrac{3}{8}\gamma_S^4\hbar^2S(S+1)[J^{(0)}(0)+10J^{(1)}(\omega_0)+J^{(2)}(2\omega_0)]\\&=\gamma_S^4\hbar^2S(S+1)c\sum_l[0.3\phi(0)+0.5\phi(\omega_0)+0.2\phi(2\omega_0)]\\&=3\gamma_S^2k_BT\chi\sum_l[0.3\phi(0)+0.5\phi(\omega_0)+0.2\phi(2\omega_0)],\end{aligned} \tag{11}$$

in the case of the electron-electron dipolar interaction.[16] The susceptibility χ is in unit of emu/(monomer unit). At the second equality of Eqs. (10) and (11) a powder average of $J^{(j)}$'s was taken, resulting in the lattice sum over r_1 and r_2 described by $\sum_l=\Sigma P_2(\cos\theta_{12})/(r_1^3r_2^3)$.[6] For the oriented samples, the first line of Eqs. (10) and (11) have to be applied.[20,21] The spin-spin relaxation rate T_2^{-1} could be observed as a broadening of the ESR linewidth $\Delta H_{pp}=2T_2^{-1}/(\sqrt{3}\gamma_S)$, and used to be written by the summation of the two terms $T_2'^{-1}\propto 0.3\phi(0)$ and $T_1'^{-1}\propto 0.5\phi(\omega_0)+0.2\phi(2\omega_0)$. The first one, the so-called secular width, three-tenths of $T_2^{-1}(0)$, is the static electron-electron dipolar broadening narrowed by the rapid diffusive motion and is independent of frequency. The second one, another seven-tenths, is produced by the rapid spin-lattice relaxation mechanism, called as a lifetime broadening and depends on the frequency in a somewhat different way from that of T_1^{-1}. In the 3D regime at $\omega\ll 1/\tau_\perp$, T_2^{-1} is expected to become equal to T_1^{-1} as was found experimentally in the pristine *trans*-polyacetylene.[22] The ESR linewidth measurement is suit-

able to study the spin dynamics because it is easier to measure with high accuracy than T_1^{-1}.

IV. RESULTS

Figures 2 and 3 show the temperature dependence of the ESR linewidth as a function of the inverse of the square-root frequency for *trans*-$(CD)_x$ and *trans*-$(CH)_x$, respectively. The solid curves show the least-squares fit of the quasi-one-dimensional diffusion described by Eq. (11). A marked difference between the two isotopic polymers, *trans*-$(CD)_x$ and *trans*-$(CH)_x$, has been found in the anomalous broadening below 6 MHz [$1/\sqrt{f} \sim 0.4$ $(\mathrm{MHz})^{-1/2}$] in *trans*-$(CH)_x$. Although data below 6 MHz in the *trans*-$(CD)_x$ are not shown in Fig. 3, angular dependence of the linewidth taken at 10 K clearly demonstrates absence of the anomalous broadening down to 3 MHz [~ 0.58 $(\mathrm{MHz})^{-1/2}$] compared with that at 18 MHz [~ 0.24 $(\mathrm{MHz})^{-1/2}$] as shown in Figs. 4(a) and 4(b). This anomalous broadening found only in *trans*-$(CH)_x$ will be discussed in the next section as one of evidences for applicability of the diffuse-trap model.

On the contrary, a common feature of Figs. 2 and 3 is a monotonous increase of the overall linewidth with decreasing temperature, together with the characteristic frequency dependence for the quasi-one-dimensional diffusion as shown by the solid curves indicating Eq. (11). Equations (11) and (10) predict that this lifetime (nonsecular) broadening, dependent on frequency, reaches up to 70% of T_1^{-1} in maximum and that the motional narrowed (secular) width, independent of frequency, amount to 30% of T_1^{-1}. This prediction has been found to be really consistent with the reported T_1^{-1} data.[22] Further, relaxation mechanisms for T_1^{-1} have been identified to the electron-electron dipolar and the hyperfine couplings from a beautiful linear correlation of T_1^{-1} with the neutral soliton concentration and isotope effect.[22] These facts suggest that not only Eq. (11), but also the second mechanism, are required for the ESR line broadening to explain Figs. 2 and 3 and it could be of static character instead of the lifetime broadening mechanism. The temperature dependence of the broadening (ΔH_{trap}) due to the second mechanism deduced from Figs. 2 and 3 is shown in Fig. 5 both for *trans*-$(CD)_x$ and *trans*-$(CH)_x$.

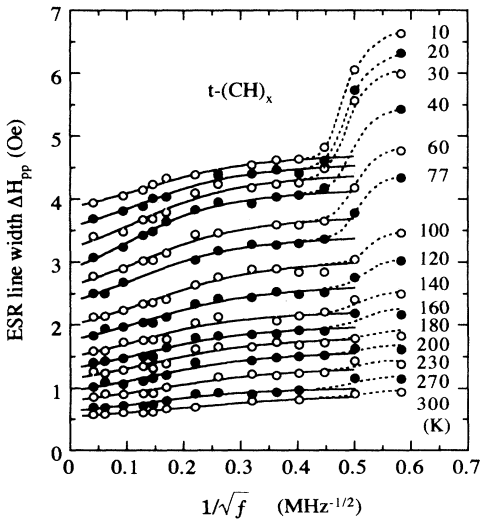

FIG. 2. The frequency dependence of the ESR linewidth for *t*-$(CH)_x$ with the implicit parameter of the temperature. Note that the anomalous line broadening is found at higher frequency than 6 MHz ($1/\sqrt{f} \approx 0.4$) only in *t*-$(CH)_x$.

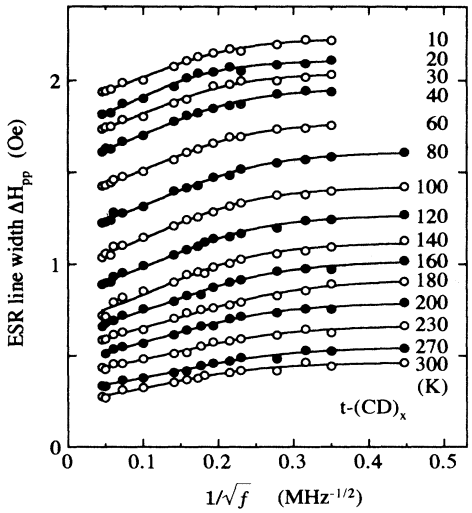

FIG. 3. The frequency dependence of the ESR linewidth for *t*-$(CD)_x$ with the implicit parameter of the temperature.

The analysis of the linewidth in terms of Eq. (11) gives us the diffusion rate $D_{\parallel}$ along the chain, the cutoff frequency $1/\tau_{\perp}$, and the temperature dependence of the secular broadening $(\gamma T_2')^{-1}$ which could be compared with the spin-echo decay rate $(\gamma T_M)^{-1}$. Figure 6 demonstrates the temperature dependence of the secular broadening for *trans*-$(CD)_x$, together with the spin-echo decay rates[9,23] $(\gamma T_M)^{-1}$ in units of Oe. This figure is another evidence for an applicability of the diffuse-trap model as will be discussed in the next section.

Figure 7 shows the temperature dependence of the diffusion rate $D_{\parallel}$ along the polyacetylene chain, together with that derived from NMR T_1^{-1}. Both of the data sets demonstrate a consistency of the analysis in terms of the diffuse-trap model for ESR and NMR, although the data show large scattering. It is noteworthy to mention that for ESR the temperature dependence of correction factors due to the trapping of the neutral soliton is entirely different from that for NMR. That is apparently quite a different temperature dependence of the diffusion rates derived from ESR and NMR without the correction, successfully converged by the trapping correction to the very similar one to each other, not only qualitatively but also quantitatively.

Figure 8 indicates the temperature dependence of the cutoff frequency for *trans*-$(CD)_x$ and *trans*-$(CH)_x$. The origin of the cutoff frequency is not necessarily unique, but some possibilities can be discussed; exchange coupling between spins,[24] real interchain hopping of neutral soliton[25] and so on. A possible source of $1/\tau_{\perp}$ in Fig. 8

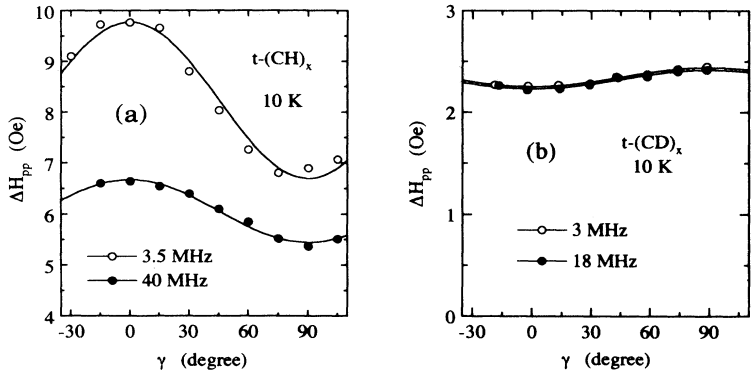

FIG. 4. The angular dependence of the ESR linewidth in (a) *trans*-$(CH)_x$ at 10 K, 40 MHz (without the excess width) and 3.5 MHz (with the excess width) and (b) *trans*-$(CD)_x$ at 10 K, 18 MHz, and 3 MHz. Note that the excess linewidth shows the same phase of pattern as that for *cis*-$(CH)_x$, the same as the width due to trapping (see text in detail).

will be examined in Sec. V F in terms of these mechanisms.

V. DISCUSSION

A. Diffuse-trap model

At the X-band frequency, the linewidth is originated first by the second mechanism shown in Fig. 5 and second by the small secular width, since the lifetime broadening occupies only a tiny part. Nechtschein *et al.* have proposed a diffuse-trap model for the mechanism of the line broadening at the X-band ESR.[12] The diffuse-trap model assumes that the neutral soliton will visit some trapping site and stay for a longer time compared with the normal sites. The resulting linewidth is the sum of the broadening originated by the two different mechanisms. The first one is the 1D diffusive motion of the neutral soliton that works dominantly when the soliton diffuses in the normal sites. It broadens the ESR line by $\Delta H_{\rm diff}(T,\omega)$ as described by Eq. (11) with a correction factor due to the trapping:

$$Q_d=[c_{\rm diff}+\sqrt{2}c_{\rm tr}]c_{\rm diff}+\sqrt{2}c_{\rm tr}c_{\rm diff}$$
$$\approx 1+1.83c_{\rm tr}-0.83c_{\rm tr}^2$$

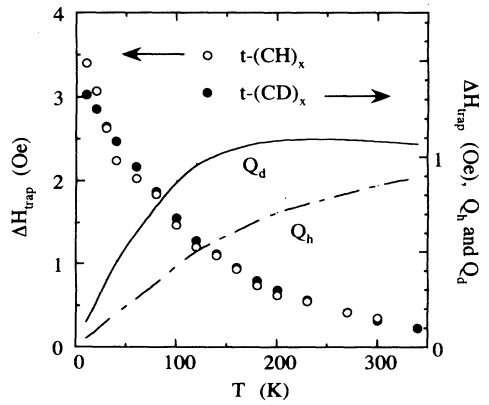

FIG. 5. The temperature dependence of the width due to trapping (the constant contribution in Figs. 2 and 3) in t-$(CH)_x$ and t-$(CD)_x$ and the correction factor of the trapping; the dashed curve, $Q_h=1-c_{\rm tr}$, and the solid curve, $Q_d=1+0.83c_{\rm tr}-1.83c_{\rm tr}^2$.

for the electronic dipolar coupling and $Q_h=c_{\rm diff}=(1-c_{\rm tr})$ for the hyperfine coupling, where $c_{\rm tr}$ is the probability for the soliton being in the trapped state and $c_{\rm diff}$ is that for the soliton diffusing. The first term in Q_d is a correction for the diffusing soliton and the second is for the trapped one. The coefficient $\sqrt{2}$ corrects the change of the effective diffusion rate from $1/\sqrt{2D_\parallel}$ for mutual diffusion to $1/\sqrt{D_\parallel}$ for one side diffusion.

On the other hand, the second mechanism works when it is in the trapped state where the static hyperfine coupling broadens the ESR linewidth by $c_{\rm tr}\Delta H_{\rm hyp}$ and the static electron dipolar coupling between the trapped solitons does it by $c_{\rm tr}^2\Delta H_{\rm dip}$ (because it needs another soliton in the trapped state). Then, the diffuse-trap model predicts

$$\Delta H_{\rm trap}(T)=c_{\rm tr}(T)\Delta H_{\rm hyp}+c_{\rm tr}^2(T)\Delta H_{\rm dip}$$

as the second static broadening mechanism. Providing that $c_{\rm tr}=1$ at $T=0$ and that the ratio of the hyperfine

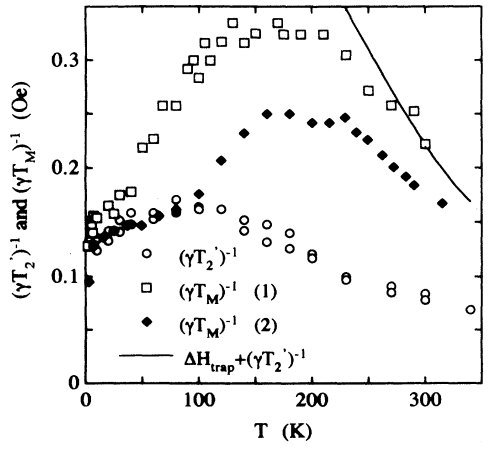

FIG. 6. The temperature dependence of the motional narrowed secular width $(\gamma T_2')^{-1}$ which is approximately equal to $(\gamma T_2)^{-1}$ at the X band [Eq. (2.11)] and the phase memory time T_M by (1) Shiren *et al.* (Ref. 9) and (2) Isoya (Ref. 23). The solid curve shows $(\gamma T_2')+\Delta H_{\rm trap}$. At temperatures lower than 100 K, $(\gamma T_M)^{-1}$ coincides with the secular width $(\gamma T_2')^{-1}\sim(\gamma T_2)^{-1}$ at the X band. At temperatures higher than 200 K, however, $(\gamma T_M)^{-1}$ is governed not only by the secular width $(\gamma T_2')^{-1}$, but also by $\Delta H_{\rm trap}$.

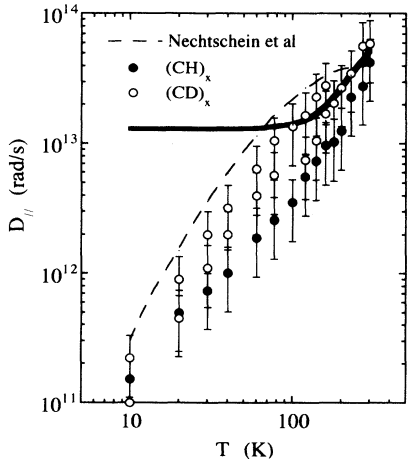

FIG. 7. The temperature dependence of the diffusion rate along the chain $D_{\parallel}$ for *t*-$(CH)_x$ (Refs. 13 and 14) together with that by ^1H NMR. The thick solid curve indicating $D_{\parallel}$ for *t*-$(CD)_x$ without the trapping correction, demonstrates that the effect due to trapping is negligibly small above 100 K.

widths[26] for *trans*-$(CD)_x$ and for *trans*-$(CH)_x$ $\Delta H_{\rm hyp}(H)/\Delta H_{\rm hyp}(D)=3.62$ as an average of isotropic and anisotropic hyperfine couplings, one can estimate $\Delta H_{\rm hyp}=0.87$ Oe for *trans*-$(CD)_x$, 3.16 Oe for *trans*-$(CH)_x$, and $\Delta H_{\rm dip}=0.54$ Oe. These values allow us to estimate the temperature dependence of $c_{\rm tr}(T)$, as shown in Fig. 5 by $Q_h=(1-c_{\rm tr})$. Such temperature dependence of $c_{\rm tr}$ has been reported to be successfully explained in terms of distributed trapping potentials from 0 to -650 K.[12]

As a result, the diffuse-trap model predicts $\Delta H_{\rm diff}(T,\omega)+\Delta H_{\rm trap}(T)$ for the cw ESR linewidth, which is described schematically in Fig. 9. If both of the line shapes are Lorentzian, one gets a simple sum of the two contributions. The observed data shown in Figs. 2 and 3 could be interpreted well by this prediction. Especially, the anomalous broadening observed only in *trans*-$(CH)_x$ below 6 MHz could also be accounted for by this

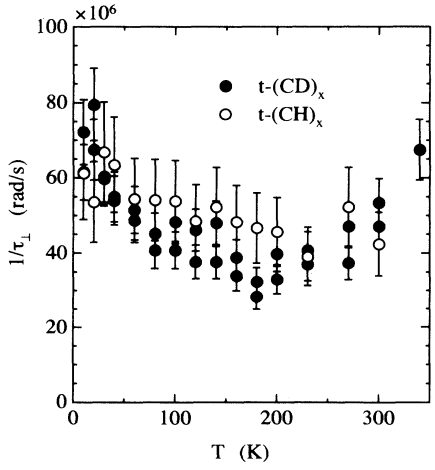

FIG. 8. The temperature dependence of the cutoff frequency $\tau_{\perp}$ for *t*-$(CH)_x$ and *t*-$(CD)_x$.

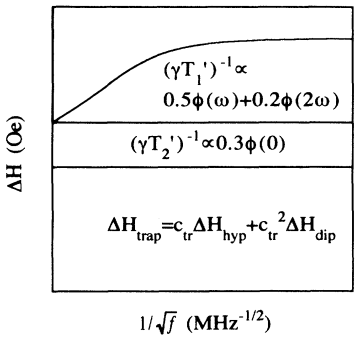

FIG. 9. A schematic figure for the ESR linewidth with the diffuse-trap model.

model and the analyzed result gives an estimate for the highest spin density of the neutral soliton as about 0.1 spin,[14] consistent with an electron nuclear double resonance (ENDOR) result.[27] In addition, the spin-echo decay rate data[9,23] are also consistent with the diffuse-trap model. Furthermore, the multiple-quantum spin coherence experiment[20] is really the most direct evidence for the presence of the trapping and for necessity to apply the diffuse-trap model to the *trans*-polyacetylene system, although it has been unreasonably interpreted by the original authors to conclude that all the spins in *trans*-polyacetylene are trapped.

B. Anomalous broadening in *trans*-$(CH)_x$

A hint to solve the origin of the anomalous broadening below 6 MHz in *trans*-$(CH)_x$ could be found in the anisotropy pattern of the linewidth plotted against the angle of the external magnetic field with an orientational direction of the stretch-aligned film as demonstrated in Figs. 4(a) and 4(b). One can easily find that the phase of the anisotropy pattern at 3.5 MHz in *trans*-$(CD)_x$ is the same as that at 40 MHz, which means that the main mechanism for the anomalous broadening is the same as that at 40 MHz. It is, however, reversed from that in *trans*-$(CD)_x$. Contrary to this, the phase of anisotropy patterns of ESR T_1^{-1} for both $(CH)_x$ and $(CD)_x$ has been found to agree with each other and could be interpreted by the relaxation mechanism due to the 1D soliton diffusion as described by Eq. (10).[20,21] This fact could be understood that in *trans*-$(CH)_x$, the linewidth was dominated by the width $\Delta H_{\rm trap}$ due to trapping, but in *trans*-$(CD)_x$, by $\Delta H_{\rm diff}$ instead of $\Delta H_{\rm trap}$ because of a small dipolar moment of deuteron. Further, T_1^{-1} is only weakly affected by $\Delta H_{\rm trap}$ in both $(CH)_x$ and $(CD)_x$.

Actually, the phase of the linewidth anisotropy observed in *cis*-$(CH)_x$ which comes from the static hyperfine broadening ($\propto \Delta H_{\rm hyp}$ appeared in Sec. V A) is the same as that in *trans*-$(CH)_x$ [Fig. 4(a)] and is reversed from $\Delta H_{\rm diff}(T,\omega)$.[28] By virtue of the small hyperfine coupling in *trans*-$(CD)_x$, the anisotropy phase of $\Delta H_{\rm diff}(T,\omega)$ surpasses that of $\Delta H_{\rm trap}(T)$, consistent with the isotope dependence of the linewidth anisotropy as shown in Figs. 4(a) and 4(b). Therefore, the anomalous increase of the linewidth below 6 MHz could be ascribed to an increase

of $\Delta H_{\rm trap}(T)$.

What happens below 6 MHz? As a conclusion the origin of the anomalous broadening in *trans*-$(CH)_x$ could be assigned to a crossover from "unlike spin" to "like spin" as decreasing the resonance frequency of ESR. Usually the hyperfine coupling between the electron spin and the nuclei is called as coupling between "unlike spins," because a large difference of Larmor frequencies for them prevents an energy conservation requirement for mutual spin flip-flop transition induced by the $BS_{\pm}I_{\mp}$ term in the dipolar Hamiltonian [the second term of Eq. (2a)].[16] Then, only the AS_zI_z term [the first term of Eq. (2a)] is effective for "unlike spins" to broaden the linewidth and both AS_zI_z and $B_{\pm}I_{\mp}$ terms are effective for "like spins." This situation would be also valid even for the electronic dipolar coupling because a decoupling condition $c_{\rm tr}\Delta H_{\rm hyp} \gg c_{\rm tr}^2 \Delta H_{\rm dip}$ holds even in *trans*-$(CD)_x$ excluding at lowest temperature where $\Delta H_{\rm hyp}(0.87\ {\rm Oe}) \approx \Delta H_{\rm dip}(0.54\ {\rm Oe})$, since $c_{\rm tr} \approx 1$.

Let us consider an effective coupling constant $a_{\rm eff}=a\rho$, where the a is the so-called hyperfine constant per one electron spin and the ρ is the spin density on the concerned carbon site. The $a_{\rm eff}$ determines a hyperfine splitting of ESR spectra. It also determines the coupling to be "like" or "unlike" following the criterion $H_0 > a_{\rm eff}$ for "unlike spins." The theoretical ratio of the excess broadening by $BS_{\pm}I_{\mp}$ to that by AS_zI_z is 0.5 which agrees very well with 0.56 ± 0.09 calculated from Fig. 2.

From this conclusion and a threshold frequency of 6 MHz as $a_{\rm eff}$, one can estimate the maximum spin density $\rho_{\rm max}$ for the neutral soliton as $\rho_{\rm max} \geq 0.1$, providing $a=-23$ (Oe/spin). This figure is consistent with the ENDOR result of $\rho_{\rm max}=0.1-0.19$ spins and/or carbon for *cis*-$(CH)_x$,[27] but is inconsistent with the uniformly delocalized wave function over from 40 to 60 carbon sites.[29] This result is good evidence for the SSH-type localized wave function for the neutral soliton both in *cis*- and *trans*-$(CH)_x$, expect for the negative spin polarization in odd carbon sites due to the Coulomb correlation.[27,30]

It was shown that the most basic parameter of ESR, linewidth, could not be understood only by the 1D diffusive motion, but it needs to take into account the effect of the neutral soliton trapping.

C. Motional narrowed (secular) width and spin-echo decay rate

The motional narrowed width $(\gamma T_2')^{-1}$ could be derived by fitting the linewidth data in Fig. 3 to Eq. (11), as shown in Fig. 6 for *trans*-$(CD)_x$ together with the spin-echo decay rate $(\gamma T_M)^{-1}$ in units of Oe, measured at the X band. The $(\gamma T_M)^{-1}$ is equal to or larger than the $(\gamma T_2')^{-1}$ from their definition as was found experimentally in Fig. 6. Below 100 K, the two different sets[9,23] of $(\gamma T_M)^{-1}$ approximately agree with the $(\gamma T_2')^{-1}$ and immediately go beyond the $(\gamma T_2')^{-1}$ above 100 K, approaching to the total ESR linewidth $\Delta H_{\rm diff}(T,\omega) + \Delta H_{\rm trap}(T)$ at the X band around 300 K. Then, let us consider how $\Delta H_{\rm trap}(T)$, which is inactive for T_1^{-1}, becomes active for the spin-echo decay rate.

Below 100 K, it is required that the average duration $t_{\rm trap}$ to stay in the trapping site has longer than T_2' by enough to make $\Delta H_{\rm trap}(T)$ a static inhomogeneous field. An effect of such constant field to T_M can be eliminated by the spin-echo pulse sequence. On the other hand, around 300 K, $t_{\rm trap}$ would be fairly shorter than T_2' to make $\Delta H_{\rm trap}(T)$ a time-dependent random field which is active for T_M. Then, at the crossover temperature, the condition $T_{\rm trap} \approx T_2' \approx 1\ \mu$s would be realized. This criterion is consistent with the appearance of the anomalous broadening below 6 MHz where the criterion $a_{\rm eff} \approx 4\times10^7 \gg 1/t_{\rm trap} \approx 10^6\ {\rm s}^{-1}$ is required to hold. Therefore, the analyzed secular width and the spin-echo decay rate are fully consistent with the diffuse-trap model.

Note that it is more difficult than the reported[9] to analyze meaningfully the spin-echo decay rate without any other information on the nature of (1) dimensionality of the spin motion which definitely control the spin-echo decay rate through $T_2'^{-1}(T) \propto \sqrt{\tau_{\perp}(T)/D_{\parallel}(T)}$, (2) the local field to be static or dynamic in interesting time scale, and (3) dynamics of the spins like soliton trapping. The present analysis of the linewidth as functions of frequency and temperature becomes possible to separate the linewidth into several factors and makes clear the spin-echo decay rate to consist of at least two different mechanisms.

D. Multiple-quantum spin coherence experiment (Ref. 11) as a direct evidence for neutral soliton trapping

An interesting, but sophisticated, discussion has been reported that all of the spins are localized in 99% ^{13}C enriched polyacetylene, studied by the multiple quantum NMR (MQNMR) detected by ESE technique.[11] It will however, be shown that this would be a clear experimental evidence demonstrating the validity of the diffuse-trap model instead.

Three pulses $\pi/2$-τ-$\pi/2$-τ_1-$\pi/2$-τ_2 were applied to the electron spin, i.e., the neutral soliton, to induce ^{13}C MQNMR transition only in nuclei coupled to the soliton. The authors have found qualitatively the same spectra for *trans*-$(CH)_x$ and *cis*-$(CH)_x$ at 4 and 298 K, demonstrating that the observed spins coherently coupled with about 13 carbon nuclei under all the studied conditions and that as a result the shape of the neutral soliton is concluded to be the same as in each isomer.

If the neutral soliton were diffusing faster than the coupling frequency between the spin and the nuclei, the multiple quantum coherence would be destroyed by decoupling of the electron-nuclear interaction. This means that the neutral soliton in the diffusing state could not be observed by this technique, but only the soliton in the trapped state could be observed, that is, the qualitative spectra of this experiment never give any suggestion on the existence of the soliton in the diffusing state, but absolute intensity will be able to do. The reason why the authors concluded "all" the spins were trapped instead of this fact was that the ESR signal composed of only a single species, which requires "the observed" MQNMR signal should be "all" of the present spins. Following the

diffuse-trap model, however, "all" of the spins have a chance to contribute to the MQNMR signal in terms of a time sharing of the diffusing and the trapped states. Therefore, the experimental result reported in Ref. 11 never demonstrates that "all" the solitons were trapped or not as insisted by the authors, but does the existence of the soliton in the trapped state even at 298 K, consistent with the diffuse-trap model of the neutral soliton in the pristine polyacetylene.[12,13] The temperature dependence of the ESR linewidth ΔH_{trap} due to trapping shown in Fig. 5 predicts that around 10% of the neutral solitons are in the trapped state even at 298 K and that "all" the solitons have a chance to join the MQNMR signal with a probability of 10%. To account for the temperature dependence of the ΔH_{trap} shown in Fig. 5, it was shown that a trapping potential with around 650 K was required.[12] Such a large trapping potential assures that the same solitons in the deepest trapping potential stay for a long enough period to join the MQNMR signal even at room temperature.

Therefore, this technique would be useful as another way to determine how many solitons are trapped at each temperature to check the diffuse-trap model quantitatively. Actually, the reported MQNMR in *trans* isomer has a higher signal-to-noise ratio than in *cis* isomer at 4 K, which is consistent with the 10–100 times higher spin concentration in the *trans* isomer than the *cis* one. At 298 K, however, the *trans* isomer shows a lower signal to noise ratio than the *cis* one, which suggests that more than 90% of neutral solitons do rapid diffusion or, in other words, in 90% of time ratio the neutral solitons diffuse rapidly. Of course, one needs to check experimental conditions carefully; the authors did not mention any information on their spin concentration in the samples and the accumulation number for each spectrum.

As a conclusion, this experiment is the direct evidence for the diffuse-trap model and could be a good quantitative test of the model, if an extremely difficult quantitative analysis were successful.

E. Relation of DNP with the diffuse-trap model

Temperature dependence of the dynamic nuclear polarization (DNP) experiment was reported at 9.3 GHz between 1.5 and 300 K for *t*-$(CH)_x$ by Clark *et al.*[7] They obtained both Overhauser (OE) and solid state (SSE) enhancements independently. The OE is characteristic for dynamic interaction between nuclear spins and electron spins, with rapid motion. On the other hand, the SSE is characteristic for static interaction between them. In the other words, observation of the pure OE is a clear evidence that the electron spin is moving with a correlation time τ comparable with $1/\omega_e$. At 300 K, the pure OE was observed,[5,7] which is really consistent with the ESR linewidth analysis reported here. With decreasing temperature, the SSE starts to mix with the OE effect. The OE and the SSE can be discriminated by the ESR frequency at which the maximum enhancement would be obtained; the same frequency as the usual ESR peak for the OE, but at $\omega_e \pm \omega_n$ for the SSE.[16] Namely, in the SSE a required energy $\hbar(\omega_e \pm \omega_n)$ for simultaneous spin flip of both nuclear and electron spins could be supplied by the r.f. irradiation instead of the spin motion. Then, if the correlation time τ of the electron spin motion becomes shorter than the inverse of the hyperfine coupling strength, the SSE will disappear because of motion decoupling and the OE starts to increase.

Therefore, the appearance of the SSE below 200 K consistently corresponds to the increase of the neutral soliton in the trapped state. The authors of Ref. 7 analyzed the peak intensity of the SSE with the electron spin trapping, quantitatively. Unfortunately, since the intensity of the SSE contains a lot of parameters to be assumed, quantitative conclusion should be taken carefully. Here, we can say that the whole data for the DNP experiments were fully consistent with the present conclusion interpreted with the diffuse-trap model. They also analyzed the OE quantitatively and obtained a conclusion that the estimated value of τ^{-1} at 300 K is less than ω_e and that the τ^{-1} is proportional to the square root of the temperature, which is not fully consistent with the present analysis. These quantitative conclusions are, however, also taken with great care, because there are some misunderstandings in their analysis as follows.

They reported a figure indicating the peak intensity for the OE (ε_0) and the SSE (ε_S) as a function of $1/\omega_n\tau$, deduced from the relations, $\varepsilon_0 \propto (\gamma_e/\gamma_n) N T_{1n} \phi(\omega_e)$ and $\varepsilon_S \propto (\gamma_e/\gamma_n) N (T_{1n}/T_{1e})$, where N is the neutral soliton concentration in the diffusive state for ε_0 and in the trapped state for ε_S, and T_{1n} and T_{1e} are the spin-lattice relaxation rate for the nuclear spins and the electron spins, respectively. Such a figure demonstrated that the OE has a peak at $1/\tau \approx \omega_e$ without showing formulations for T_{1n} and T_{1e} and $\phi(\omega_e)$ for the 1D and 3D cases. However, ε_0 does not show any dependence on the correlation time in the limit of $1/\tau \gg \omega_e$.[16,22] It can be easily shown that ε_0 has no peak at $1/\tau \approx \omega_e$:

$$\varepsilon_0 \propto (\gamma_e/\gamma_n) T_{1n} \phi(\omega_e)$$

$$\approx (\gamma_e/\gamma_n) \sqrt{\omega_n/\tau} \sqrt{\omega_e/\tau} = \sqrt{\gamma_e/\gamma_n}$$

for the 1D case and unity for the 3D case with an exponential type correlation.[16] This difference between the 1D and the 3D cases is originated by a frequency dependence of $\phi(\omega) \propto 1/\sqrt{\omega/\tau}$ which is characteristic for the 1D case and enhances $1/T_{1n}$ by $\sqrt{\gamma_e/\gamma_n}$ from the 3D case. This enhancement leaks a transferred magnetization from the electron spin to the lattice. It is required to reconsider all the quantitative analysis in Ref. 7, since the quantitative discussion was based on the observation that there is no peak in ε_0.

On the contrary to a discussion in Ref. 7 in the regime of $\omega_n \ll 1/\tau \ll \omega_e$, the enhancement of the DNP depends on the dimensionality of the motion. One gets $\varepsilon_0 \propto \sqrt{\omega_n/\omega_e^2 \tau_\perp}/(\omega_e\tau)$ with a general relation for the quasi-1D case,[31] and $1/(\omega_e\tau)^2$ for the 3D case. Note that ε_0 depends not only τ but also $\tau_\perp$, which increases the difficulty to analyze ε_0 quantitatively only with the OE result. In both the 1D and the 3D cases, ε_0 approaches to a small enough value $\gamma_n/\gamma_e \approx 0$ at $1/\tau \leq \omega_n$.

As a conclusion of this section, the DNP data are qual-

itatively consistent with the present ESR linewidth analysis with the diffuse-trap model. Unfortunately, however, a quantitative analysis is difficult only with the DNP data, since one could not get any lower limit of the correlation time from ε_0 due to absence of dependence on τ^{-1} at $\tau^{-1} \gg \omega_e$.

F. Temperature dependence of diffusion rate and cutoff frequency

One of the quantitative results of the ESR linewidth analysis is the temperature dependence of the diffusion rate $D_\parallel$ along the chain and the cutoff frequency $1/\tau_\perp$ which is, in some case, equal to the interchain hopping rate $D_\perp$ of the spins. The three data sets for $D_\parallel$ are compared in Fig. 7 as a function of the temperature, obtained by the analysis in terms of the diffuse-trap model. A power-law behavior T^n with $n \sim 2$ is a common feature of these data sets in spite of large scattering of the data. The positive coefficient of the temperature dependence $\partial D_\parallel / \partial T > 0$ suggests that there is some weak but finite localizing potential for the neutral soliton and a driving force of the neutral soliton diffusion is of phonon scattering. Detailed theoretical considerations of the neutral soliton in the *trans*-polyacetylene have been reported from different approaches.[32,33]

A different temperature dependence of the diffusion rate $D_\parallel$ along the chain has been reported by analyzing the spin-lattice relaxation rate T_1^{-1} of ESR in the *trans*-polyacetylene.[8] They discussed that the neutral soliton diffusion is of ballistic motion limited by a phonon scattering like a conduction electron in the metals, to account for the increasing temperature dependence rapidly until 100 K and gradually above 100 K.[8] This looks like a natural interpretation, if one has only the ESR T_1^{-1} data. Now we need, however, to take account of the neutral soliton trapping which is required from the conclusion of the ESR linewidth analysis for single Lorentzian (single species of ESR) as follows; the anomalous broadening below 6 MHz in *trans*-$(CH)_x$, the angular dependence of both T_1^{-1} and the linewidth in the stretch aligned samples, and the residual ESR linewidth interpreted as the width due to trapping. The experiments like the ESR T_1^{-1}, the spin-echo decay rate T_M^{-1}, and the free-induction decay shape of the electron spin magnetization could be analyzed with any desirable assumptions without self-restricting prerequisite assumption consistent with the ESR linewidth, resulting in a variety of conclusions for the temperature dependence of the diffusion rate. But the basic parameter of the ESR, the linewidth requires the trapping of the neutral soliton as a natural results or some equivalent mechanisms to account for the data shown in Figs. 2–5.

Therefore, we would like to stress that these experiments are required to analyze with the assumption which are consistent with the ESR linewidth, since these physical quantities including the linewidth are not independent of the others. The present linewidth analysis consists of not only the width due to trapping, but also the ESR T_1^{-1} and the ESR T_M^{-1} through ${T_1'}^{-1}$ and ${T_2'}^{-1}$. As a result, within the diffuse-trap model it is demonstrated that the present analysis is consistent with the spin-echo decay rate as discussed in Sec. V C, the free-induction decay shape which is the Fourier transform of the ESR linewidth, the multiple quantum NMR (Sec. V D), the dynamic nuclear polarization (Sec. V E) and the ESR T_1^{-1} at least around room temperature including low frequencies down to 5 MHz. Here, we could mention on the ESR T_1^{-1} that the rapid decrease with decreasing temperature below 100 K is naturally interpreted in terms of a suppression effect of ESR T_1^{-1} caused by (1) a delocalized wave function for the neutral soliton[19] accompanied by the steep decrease of the on-chain diffusion rate $D_\parallel$ demonstrated in Fig. 7 and (2) a decrease of the number of the diffusing soliton.

The cutoff frequency shows a weak temperature dependence with a minimum around 200 K as shown in Fig. 8. Since the diffusion rate $D_\perp$ across the chains is equal to or smaller than the cutoff frequency, an anisotropy of the diffusion rate is fairly large, ranging from $\geq 3 \times 10^3$ at 4.5 K to $\geq 8 \times 10^5$ at 300 K. Such anisotropic diffusion in the *trans*-polyacetylene is consistent with the topological nature of the neutral soliton. Although highly one-dimensional diffusion looks inconsistent with the observed Lorentzian line shape, which is usually expected for the three-dimensional system, it can be shown to be consistent with the observed Lorentzian in the case of the larger cutoff frequency than the ESR linewidth.[34]

The temperature dependence of the $1/\tau_\perp$ is explainable qualitatively as follows. In the temperature range below 100 K, the exchange interaction between the solitons would govern $\tau_\perp$; at the lowest temperature most of the neutral solitons are trapped, probably several solitons gathering around the adsorbed oxygen on the surface of fibril, which enhances the exchange interaction between them as an origin of the $1/\tau_\perp$.[24] With increasing the temperature, the neutral solitons start to diffuse rapidly, which decrease the efficiency of the exchange interaction between the neutral solitons. In the higher temperature range, the neutral soliton hopping via the charged solitons assisted by phonon would become dominant. Kivelson has suggested a strong temperature dependence for the conductivity $\sigma \propto T^{13}$ in this mechanism, which is similar to the rapid increase of $\mathcal{D}_\perp$ around room temperature.

VI. CONCLUDING REMARKS

Many tries to reveal the dynamics of the spins in the *trans*-polyacetylene were reported and remained many conclusions, equivalently many discrepancies to be solved. Here, one try has been reported to elucidate the reported ESR experiments in terms of the diffuse-trap model, successfully. There is a standpoint that the diffuse-trap model is not necessarily required to understand the pulsed ESR experiments. In that case, the many experimental data, closely related to the ESR spin-lattice relaxation rate and the spin-echo decay rate, shown in Figs. 2–5, have to be explained by each applied model to keep self-consistency.

The ESR linewidth analysis technique has been shown to be powerful and useful for the spin-dynamics study and has recently been applied to the conducting polymers to light up the dynamics of the spin and charge carrier,

reflecting charge conduction in the polymer chains including a microscopic anisotropy of carrier motion.[34–40]

ACKNOWLEDGMENTS

The author (K.M.) would like to thank Professor J. Isoya for providing unpublished data on the spin-echo-decay rate and S. Komukai for ESR measurements of *trans*-$(CH)_x$. He also thanks M. Suezaki for preparing highly oriented polyacetylene sample. This work was supported in part by Grant-in-Aid for Scientific Research (C) from the Ministry of Education, Science and Culture (No. 03640321).

*Present address: Dept. Phys., Chuo University, Bunkyo-ku, Tokyo, 112 Japan.

[1]For a recent development, see, for example, Proceedings for International Conference on Science and Technology of Synthetic Metals 1988 (ICSM '88), Sante Fe, 1988 [Synth. Met. **27-29** (1989)]; ICSM '90, Tübingen, 1990 [Synth. Met. **41-43** (1991)]; ICSM '92, Göteborg, 1992 [Synth. Met. **55-57** (1993)].

[2]W. P. Su, J. R. Schrieffer, and A. J. Heeger, Phys. Rev. B **22**, 2099 (1980).

[3]B. R. Weinberg, E. Ehrenfreund, A. Pron, A. J. Heeger, and A. G. MacDiarmid, J. Chem. Phys. **72**, 4749 (1980).

[4]M. Nechtschein, F. Devreux, R. L. Greene, T. C. Clarke, and G. B. Street, Phys. Rev. Lett. **44**, 356 (1980).

[5]M. Nechtschein, F. Devreux, F. Genoud, M. Guglielmi, and K. Holczer, J. Phys. (Paris) Colloq. **44**, C3-209 (1983).

[6]K. Holczer, J. P. Boucher, F. Devreux, and M. Nechtschein, Phys. Rev. B **26**, 1051 (1981).

[7]W. G. Clarke, K. Glover, G. Mozurkewich, S. Etemad, and M. Maxfield, Mol. Cryst. Liq. Cryst. **117**, 447 (1985).

[8]B. H. Robinson, J. M. Schurr, A. L. Kwiram, H. Thomann, H. Kim, A. Morrobel-Sosa, P. Bryson, and L. R. Dalton, J. Phys. Chem. **89**, 4994 (1985).

[9]N. S. Shiren, Y. Tomkiewicz, T. G. Kazyaka, and A. R. Taranko, Solid State Commun. **44**, 1157 (1982).

[10]J. Tang, C. P. Lin, M. K. Bowman, J. R. Norris, J. Isoya, and H. Shirakawa, Phys. Rev. B **28**, 2845 (1983).

[11]H. Thomann, H. Jin, and G. L. Baker, Phys. Rev. Lett. **59**, 509 (1987).

[12]M. Nechtschein, F. Devreux, F. Genoud, M. Guglielmi, and K. Holczer, Phys. Rev. B **27**, 61 (1983).

[13]K. Mizoguchi, K. Kume, and H. Shirakawa, Synth. Met. **17**, 439 (1987).

[14]K. Mizoguchi, S. Komukai, T. Tsukamoto, K. Kume, M. Suezaki, K. Akagi, and H. Shirakawa, Synth. Met. **28**, D393 (1989).

[15]T. Ito, H. Shirakawa, and S. Ikeda, J. Polym. Sci. Polym. Chem. Ed. **12**, 11 (1974).

[16]A. Abragam, *Principles of Nuclear Magnetism* (Oxford University Press, Oxford, 1961), Chap. 8.

[17]G. Soda, D. Jerome, M. Weger, J. Alizon, J. Gallice, H. Robert, J. M. Fabre, and L. Giral, J. Phys. (Paris) **38**, 931 (1977).

[18]K. Mizoguchi, Makromol. Chem., Macromol. Symp. **37**, 53 (1990).

[19]F. Devreux, Phys. Rev. B **25**, 6609 (1982).

[20]K. Mizoguchi, K. Kume, S. Masubuchi, and H. Shirakawa, Solid State Commun. **59**, 465 (1986).

[21]K. Mizoguchi, K. Kume, S. Masubuchi, and H. Shirakawa, Synth. Met. **17**, 405 (1987).

[22]K. Mizoguchi, K. Kume, and H. Shirakawa, Solid State Commun. **50**, 213 (1984).

[23]J. Isoya (private communication).

[24]C. Jeandey, J. P. Boucher, F. Ferrieu, and M. Nechtschein, Solid State Commun. **23**, 673 (1977).

[25]S. Kivelson and A. J. Heeger, Synth. Met. **22**, 371 (1988).

[26]For the Fermi contact isotropic interaction $\Delta H_{\rm iso}(H)/\Delta H_{\rm iso}(D)=\gamma_H I_H/\gamma_D I_D=3.25$ and for the electron-nuclear dipole anisotropic interaction $\Delta H_{\rm ani}(H)/\Delta H_{\rm ani}(D)=\gamma_H\sqrt{I_H(I_H+1)}/\gamma_D\sqrt{I_D(I_D+1)}=3.99$ are used to estimate the average ratio providing $|\Delta H_{\rm iso}|\approx|\Delta H_{\rm ani}|$ as discussed in J. R. Morton, Chem. Rev. **64**, 453 (1964).

[27]S. Kuroda and H. Shirakawa, Phys. Rev. B **35**, 9380 (1987).

[28]S. Kuroda, M. Tokumoto, N. Kinoshita, and H. Shirakawa, J. Phys. Soc. Jpn. **51**, 693 (1982).

[29]H. Thomann, L. R. Dalton, M. Grabowski, and T. C. Clark, Phys. Rev. B **31**, 3141 (1985).

[30]M. Mehring, A. Grupp, P. Höfer,and H. Käss, Synth. Met. **28**, D399 (1989).

[31]P. K. Kahol, M. Mehring, and X. Wu, J. Phys. (Paris) **46**, 163 (1985).

[32]Y. Wada, Prog. Theor. Phys. Suppl. **113**, 1 (1993).

[33]S. Jeyadev and E. M. Conwell, Phys. Rev. B **36**, 3284 (1987).

[34]K. Mizoguchi and K. Kume, Solid State Commun. **89**, 971 (1994).

[35]K. Mizoguchi, M. Nechtschein, J.-P. Travers, and C. Menardo, Phys. Rev. Lett. **63**, 66 (1989).

[36]K. Mizoguchi, M. Nechtschein, J. P. Travers, and C. Menardo, Synth. Met. **29**, E417 (1989).

[37]K. Mizoguchi, M. Nechtschein, and J. P. Travers, Synth. Met. **41**, 113 (1991).

[38]K. Mizoguchi, M. Honda, S. Masubuchi, S. Kazama, and K. Kume, Jpn. J. Appl. Phys. **33**, L1239 (1994).

[39]K. Mizoguchi, H. Sakurai, F. Shimizu, S. Masubuchi, and K. Kume, Synth. Met. **68**, 239 (1995).

[40]F. Shimizu, Dr. thesis, Faculty of Science, Tokyo Metropolitan University, Tokyo, 1994 (unpublished).